

# Advances in Time-Resolved Approaches To Characterize the Dynamical Nature of Enzymatic Catalysis

Robert Callender\*<sup>†</sup> and R. Brian Dyer\*<sup>‡</sup>

Department of Biochemistry, Albert Einstein College of Medicine, 1300 Morris Park Avenue, Bronx, New York 10461, and C-PCS, MS J567, Chemistry Division, Los Alamos National Laboratory, Los Alamos, New Mexico 87545

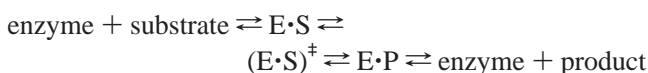
Received December 8, 2005

## Contents

1. Introduction	3031
2. Review of Time-Resolved Approaches	3032
2.1. Laser-Induced Temperature-Jump (T-jump)	3032
2.2. Time-Resolved Spectroscopic Probes	3034
2.3. Laser-Induced pH-Jump	3035
2.4. Rapid Mixing Methods	3036
3. Specific Studies	3037
3.1. Triosephosphate Isomerase (TIM)	3037
3.1.1. Triosephosphate Isomerase (TIM)—A Laser-Induced T-Jump Study	3037
3.1.2. Triosephosphate Isomerase (TIM)—Comparison of Time-Resolved Results to NMR Relaxation Studies	3038
3.2. Lactate Dehydrogenase (LDH)—Laser-Induced T-Jump Studies	3038
3.2.1. Formation of the LDH/NADH Complex	3038
3.2.2. Formation of the Michaelis Complex in LDH	3039
3.2.3. Kinetic Processes Associated with On-Enzyme Chemistry and Conformational Changes in LDH	3039
3.3. Hydride Transfer in Transhydrogenase—Continuous Flow Rapid Mixing To Resolve the Hydride Transfer Step	3040
3.4. Hydrolysis Reaction of the Ras Protein—The Use of Caged Compounds	3040
3.4.1. Time-Resolved Crystallographic Studies	3040
3.4.2. Time-Resolved FTIR Studies	3040
4. Acknowledgment	3041
5. References	3041

## 1. Introduction

The simplest kinetic pathway that describes enzymatic catalysis is



While this model tends to describe the observed kinetics in many cases, the actual chemical pathway for the enzyme

catalyzed conversion of “substrate” to “product” is believed to be substantially more complicated. Although the specific structures, viewed as a static collection of atomic positions, are important to understand to how enzymes work, the specific motions of these atoms also play a crucial role, a notion that can at least be traced back to Koshland’s “induced-fit” hypothesis.<sup>1</sup> The on-enzyme catalyzed chemistry involves considerable and specific atomic motion of both the atoms of the bound substrate and the atoms of the protein along the reaction coordinate. The types of motions involved with the chemistry are many: from the physical necessity of binding pocket atoms relaxing to accommodate the new electrostatic and steric nature of the product species compared to the substrate on one hand to conjectured “promoting vibrations” of the protein, helping to facilitate catalysis due to atomic motion within the protein along the reaction coordinate, on the other hand. Likewise, just how an enzyme binds its ligands to form the “Michaelis complex”, the specific pathway(s), the time ordering of events, and the motions of the atoms and groups of atoms involved in the binding process are all largely uncharacterized and not understood. The reason for this is that these dynamical processes cover a wide range of time scales: small scale displacements of atoms take place from picoseconds to nanoseconds; activated motions of molecular groups, such as loop motion, occur within nanoseconds to microseconds; the motions of protein domains or smaller scale group motions with high activation energies are observed on the millisecond time scale or longer. Experimental and theoretical/computational methods are just now being developed that can adequately cover this broad time range of atomic motions.

The subject of this review is a discussion of “time-resolved” approaches to the characterization of the dynamical nature of enzymatic catalysis and their application to specific enzyme systems. In fact, our goal is vastly more modest than that. Time-resolved studies of enzymes are a very old story, in some sense dating to more than 100 years ago with the success of the Michaelis–Menton description of enzyme kinetics.<sup>2</sup> Approach development has been crucial toward the goal of a determination of the time evolution of atomic structure. For example, the stopped-flow approach, as introduced several decades ago,<sup>3,4</sup> is able to reach a time resolution of a few milliseconds while the T-jump relaxation methods pioneered by Eigen and DeMaeyer using rapid capacitance discharge to produce Joule heating in conducting solutions<sup>5</sup> reached the microsecond time scale and were applied to many enzyme systems especially in the 1960s and 1970s (e.g., see refs 6–8). For probes of evolving structure,

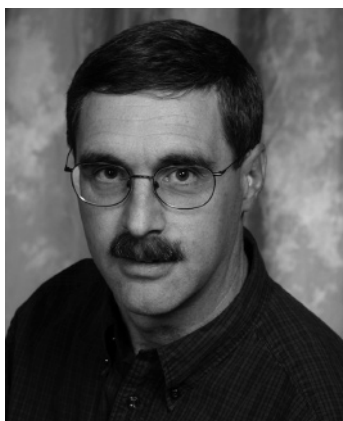
\* To whom correspondence should be addressed. E-mail: call@aecom.yu.edu (R.C.); bdyer@lanl.gov (R.B.D.).

<sup>†</sup> Albert Einstein College of Medicine. Phone: 718-430-3024. Fax: 718-430-8666.

<sup>‡</sup> Los Alamos National Laboratory. Phone: 505-667-4194. Fax: 505-667-0851.



Robert Callender has been Professor of Biochemistry at Albert Einstein College of Medicine since 1996. He received his Ph.D. from Harvard University in Applied Physics in 1969. After a year of postdoctoral studies in solid-state physics in 1969–1970 at the University of Paris, he joined the physics faculty at The City College of New York in 1970, where he became Distinguished Professor of Biophysics in 1989. He joined the faculty at Albert Einstein in 1996. The focus of his studies has been spectroscopic studies of structure and dynamics of proteins using advanced approaches. His studies have included work on the photophysics of visual pigments and, more recently, enzymatic catalysis and protein folding. He developed sensitive difference spectroscopy to characterize the vibrational structures of enzymes and fast initiation methods to probe the dynamical nature of enzymes and the kinetics of protein folding.



R. Brian Dyer received his Ph.D. degree in physical–inorganic chemistry from Duke University in 1985. Following a postdoctoral appointment at LANL in bioinorganic chemistry (with Woody Woodruff), he became a staff member in 1987. He was appointed a Laboratory Fellow in 2003. His science interests include transition metal photochemistry and photophysics, bioinorganic chemistry, metalloenzymes, O<sub>2</sub> activation (cytochrome *c* oxidase and photosystem II), protein dynamics, and protein folding. In addition to these scientific interests, he has been active in developing new approaches to the study of dynamic processes, including time-resolved laser and spectroscopic techniques, fast reaction initiation methods, microfluidics, and molecular imaging. He pioneered the development of time-resolved infrared spectroscopy and laser initiation methods and their applications to the study of protein dynamics.

enzymologists have typically relied on optical absorption and emission. Over the past decade or so, there have been substantial advancements in extending both the time resolution and range of kinetics studies as well as an expanded set of structural probes. It is these advancements that is the topic of this review. Much of the review covers work in the authors' labs, since it has been our interest to “marry” advanced approaches to investigate the dynamics of proteins in general and enzymes specifically.

Because of the importance of protein dynamics to how they function (and indeed other biological macromolecules

and complex systems), there is a substantial amount of work ongoing in many different communities to address the problem of determining dynamics, the evolution of atomic and molecular structure as a function of time. The development of computational approaches is reviewed in this issue.<sup>9</sup> Much recent progress has been made using NMR relaxation spectroscopy, which can characterize atomic motions on fast (picosecond–nanosecond) and slow (microsecond–millisecond) time scales; this approach has received recent reviews.<sup>10–12</sup> Single molecule techniques are beginning to find application in understanding the dynamical nature of enzymatic catalysis (e.g., refs 14 and 15).

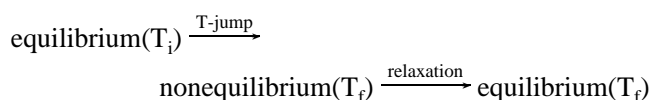
The essential feature of “time-resolved” studies is the use of a trigger method to initiate chemical or structural changes in a system, combined with a structural probe, typically spectroscopic, which follows the evolution of the system in time. For example, the fast dynamics of a limited set of proteins have been studied using pulsed laser excitation methods. These studies have focused on proteins with an absorbing prosthetic group such as heme (e.g., refs 16–21), retinal (e.g., ref 22) or chlorophyll (e.g., ref 23), because the chromophore provides a convenient means to both initiate and probe the dynamics. Generally, these experiments pump an electronic state of the chromophore, leading to photochemistry, conformational changes, or electron transfer; the response of the chromophore is probed using techniques which report primarily on the prosthetic group and only indirectly on the protein itself (e.g. transient UV/vis absorbance) (see e.g., ref 22).

Other rapid initiation methods recently developed do not rely on photoexcitation of a chromophoric prosthetic group; these include laser-induced temperature-jump (T-jump),<sup>24–28</sup> laser initiated electron transfer,<sup>29</sup> photolytic release of caged reagents such as ATP,<sup>30</sup> GTP,<sup>31–34</sup> and Ca<sup>2+</sup>,<sup>35</sup> and submillisecond rapid mixing techniques.<sup>36–39</sup> In contrast to the specialized optical trigger approaches, these techniques are much more generally applicable. It will be evident below that atomic motion can be followed by spectroscopic techniques with structural specificity over a wide time range, from picoseconds to minutes, given a suitable initiation of chemical or structural evolution. We review these “triggering” approaches below and describe the accompanying spectroscopic probes of evolving structure. There has been much progress in time-resolved crystallographic studies, and we do not discuss that here. The subject is well reviewed in several recent references,<sup>40–42</sup> including one describing time-resolved studies in protein crystals by Raman spectroscopy.<sup>43</sup>

## 2. Review of Time-Resolved Approaches

### 2.1. Laser-Induced Temperature-Jump (T-jump)

The laser-induced T-jump technique is the most versatile and simplest of the fast initiation approaches. This technique perturbs the equilibrium point of interconverting chemical species by rapidly changing the temperature, forcing the system to establish a new equilibrium point:



The use of fast T-jump methods to displace chemical equilibrium and measure relaxation rates was pioneered by

Eigen and DeMaeyer, using rapid capacitance discharge to produce Joule heating in conducting solutions.<sup>5</sup> Faster T-jumps are possible using pulsed laser excitation, usually pumping the near-infrared solvent (H<sub>2</sub>O or D<sub>2</sub>O) absorbance. This approach was first developed for studying conformational kinetics of inorganic complexes.<sup>44</sup> Vibrational relaxation takes place on the picosecond time scale both in water and in proteins; therefore, complete thermalization of solvent and solute can occur within 10–20 ps.<sup>45,46</sup> By judicious choice of temperature and solution conditions, the equilibrium of an enzyme reaction can be poised at any point. A change in temperature perturbs the equilibrium in a desired direction, and the relaxation kinetics of the system is then measured as it approaches the new equilibrium. This approach is applicable to virtually all biomolecules, and it does not necessarily require the introduction of extraneous reagents into the system.

Application of the T-jump approach to the study of enzyme reactions relies on the existence of an enthalpic difference between the old and new equilibrium points. It can be shown (e.g., refs 8 and 47) that the change in equilibrium between two interconverting species for a T-jump of magnitude  $\Delta T$  is given by

$$(\Delta K/K) = (5.67 \times 10^{-3})\Delta H\Delta T$$

where  $K$  is the equilibrium constant,  $\Delta H$  is the enthalpy difference between the two species (in kcal/mol), and  $\Delta T$  is the temperature jump (in degrees kelvin). Hence, in general, species which exist only in trace amounts will be difficult to observe. Furthermore, this approach relies on at least a small enthalpic difference between various species of the chemical system.

Analysis of T-jump kinetics requires a kinetics model in order to relate the observed relaxation times to the rate constants of the model reaction.<sup>48,49</sup> The simplest case is the relaxation between two interconverting species. One relaxation time is observed which is the sum of the forward and reverse rate constants. Both rate constants can be derived from the observed relaxation rate given the equilibrium constant for the reaction. Bimolecular reactions can be distinguished from unimolecular reactions by making measurements as a function of concentration, as demonstrated in the studies described below. In general, a minimal kinetic model requires that the number of species be equal to one more than the number of observed relaxation times. Complicated reaction schemes can be solved numerically. A general approach in which the rate equations are linearized has been worked out in substantial detail for small perturbations from equilibrium.<sup>8,47–49</sup> This approach reduces the kinetic analysis to an eigenvalue/eigenvector problem that can be solved analytically, with the eigenvalues being the relaxation times as functions of the rate constants of the kinetics model. T-jumps of 10–20 °C are too large to assume routinely that the equations can be linearized. However, analytical solutions and simulations comparing solutions from a linearized approach to numerical solutions of the nonlinear equations have shown that, often, the error is small even for T-jumps of this magnitude.

A number of approaches have been used to achieve laser-induced T-jumps. Initial attempts to produce T-jumps used laser wavelengths that are not efficiently absorbed by water, such as the 1.064  $\mu\text{m}$  fundamental of Nd:YAG<sup>50</sup> or Raman shifted pulses at 1.41  $\mu\text{m}$ .<sup>51</sup> This approach was not very successful, as only very small temperature jumps are

produced. Others used specialized lasers such as Ho:YAG<sup>52</sup> or atomic iodine<sup>53</sup> which lase at wavelengths that are strongly absorbed by water. The indirect approach of pumping a heater dye has also been used in aqueous solvents to achieve a significant temperature jump.<sup>54</sup> The magnitude of the T-jump achieved with this approach was limited to a few degrees, with the obvious additional disadvantage of possible interferences (chemical and optical) caused by the heater dye.

Our approach to the impulsive heating of a protein solution is direct pumping of the near-infrared absorbance of water (near 1.54  $\mu\text{m}$  for H<sub>2</sub>O or 1.91  $\mu\text{m}$  for D<sub>2</sub>O).<sup>55</sup> Specifically, the pump pulse is generated by Raman shifting the fundamental of a Q-switched Nd:YAG laser (one Stokes shift in methane or hydrogen, respectively) to yield a 10 ns heating pulse. The wavelength of the heating pulse lies near the peak of either the weak H<sub>2</sub>O (1.54  $\mu\text{m}$ ) or D<sub>2</sub>O (1.91  $\mu\text{m}$ ) IR absorption band ( $\sigma \approx 5\text{--}10\text{ cm}^{-1}$ ). These wavelengths were chosen because they are only moderately absorbed (about 10% typically in our cells). This ensures uniform heating of the sample within the interaction volume. Also, this frequency is ideal for our purpose because proteins absorb neither at 1.54  $\mu\text{m}$  (about 6500  $\text{cm}^{-1}$ ) nor at 1.91  $\mu\text{m}$  (about 5200  $\text{cm}^{-1}$ ). The typical energy densities we employ are 10–70 mJ per pulse focused to a 200–2000  $\mu\text{m}$  diameter spot size, which produces a 10–30 °C temperature jump.

Figure 1 shows a schematic of the nanosecond T-jump instrument using IR absorption to probe the kinetic re-

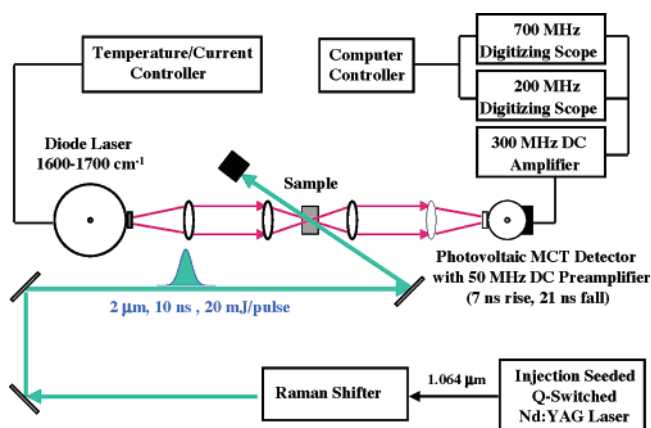


**Figure 1.** Laser-induced T-jump relaxation spectrometer using IR absorption as a probe. The time response is 20 ns to 10 ms, and by varying the laser diodes, the total frequency range spanned by this system is 900–3200  $\text{cm}^{-1}$ .

sponse.<sup>55</sup> The fluorescence T-jump instrument is not shown, but the essence of the two instruments is the same. A continuous laser beam, whose wavelength lies either in the IR or the UV/vis, irradiates the sample. The change in signal induced by the T-jump (transmission for IR or backscattered fluorescence light) is detected in real time; hence, a very accurate baseline is automatically provided, and quite small changes can be determined. The continuous wave, lead-salt, infrared diode laser shown in Figure 1 is the one chosen for IR output at 1600–1700  $\text{cm}^{-1}$  to cover the protein amide I vibrations. Other frequencies are available to cover various functional groups, including important substrate and active site groups such as carboxylic acid (1700–1760  $\text{cm}^{-1}$ ) and carboxylate (1520–1590  $\text{cm}^{-1}$ ) modes, imidazole modes (1400–1500  $\text{cm}^{-1}$ ), and phosphate modes (980–1050  $\text{cm}^{-1}$ ). The probe light for the UV/vis absorption and emission measurements is a CW argon or krypton ion laser. A number of output frequencies are available between the two lasers,

and the entire UV/vis range is well spanned. In particular, the argon ion laser running in the deep UV, which puts out light at several wavelengths from 275 to 305.6 nm, can be used to excite Trp and Tyr fluorescence,<sup>56,57</sup> or the near UV at 360 nm is used to pump the reduced ring of NAD(P)H.<sup>56</sup> Several wavelengths spanning the visible region are also available from these lasers. The temperature change induced by the T-jump in the UV/vis emission and absorption relaxation spectrometers is determined by the changes in absorption of IR light produced by a photodiode passing through the laser interaction volume (optics not shown). The UV/vis absorption arrangement (not shown) is the same as that for the IR absorption spectrometer except that a frequency tunable arc lamp is used as the probe source.

We have characterized the laser-induced T-jump produced with both nanosecond and picosecond pump pulses using time-resolved IR spectroscopy. The temperature dependence of the mid-IR spectrum of D<sub>2</sub>O serves as an internal thermometer to map the temporal and spatial profiles of the T-jump. The IR response of the D<sub>2</sub>O spectrum to a temperature change was determined from equilibrium FTIR spectra as a function of temperature. In the amide I region, from 1600 to 1700 cm<sup>-1</sup>, there is an increase in the absorption of D<sub>2</sub>O with temperature. The absorbance change is linear, with a nearly constant slope of  $3 \times 10^{-3}$  OD/°C (100 μm path length) over this whole spectral region. This absorbance change can be used to characterize the dynamics of the T-jump. Figure 2 shows the kinetic mid-IR response

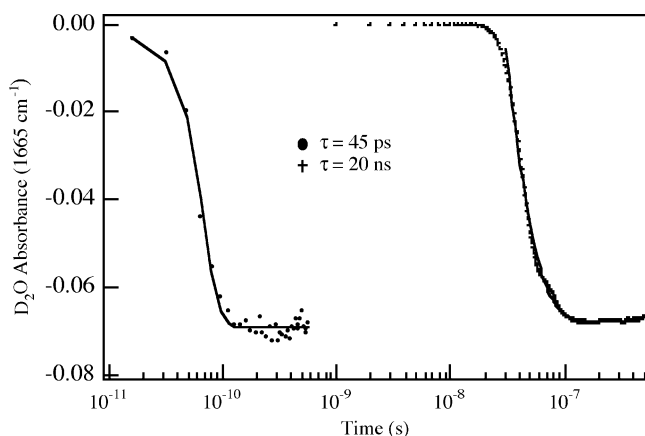


**Figure 2.** Laser-induced T-jump response of D<sub>2</sub>O absorbance at 1665 cm<sup>-1</sup>. The “pump” heating pulses are 40 ps and 15 ns, respectively.

to a T-jump produced in a D<sub>2</sub>O solution pumped with ca. 40 ps and 15 ns heating pulses. The probe wavelength of these particular traces was 1665 cm<sup>-1</sup>, although an identical kinetic response is obtained at other wavelengths. The rise time of the kinetic response is 45 ps and 20 ns, respectively, which simply follows the instrument response function in each case. It is clear that the energy deposited by the pump pulse is thermalized, and the T-jump is complete even on the earliest time scale that we can measure with our ultrafast IR setup. The decay (not shown) of the T-jump occurs on the millisecond time scale, dominated by the transfer of heat from the interaction volume to the cell windows. The magnitude of the temperature jump can be determined from the magnitude of the absorbance change and the established (from the FTIR data) linear dependence of the absorbance on temperature. The data shown in Figure 2 correspond to about a 12 °C T-jump in both cases. This experimentally

determined (calibrated) temperature rise is in excellent agreement with what we calculate for the theoretical expectation, based on the measured interaction volume and pump absorbance, and the literature values of the density and specific heat of water.

Finally, there are some potential pitfalls of the laser-induced T-jump approach outlined above. The limited laser pulse energy available at the appropriate infrared wavelength combined with the energy-to-volume ratio required to produce a reasonable T-jump greatly restricts the interaction volume. High spatial mode quality and minimal optical aberrations are required to achieve the required beam quality and interaction volume. Strong focusing conditions can also produce many undesirable effects; with short (5 ps) pulses, nonlinear effects such as self-focusing, water breakdown, and continuum generation are possible. With both picosecond and nanosecond pulses, photothermal effects such as cavitation and shock waves are possible. Fortunately, all of these effects have characteristic thresholds that usually lie well above the energy density required to produce a T-jump of reasonable magnitude (10–20 °C). The photothermal/cavitation effects also produce easily identifiable signatures in the time-resolved experiments<sup>58</sup> and can be avoided by decreasing the energy density or by changing the optical alignment. We have found that thoroughly degassing the samples is crucial in avoiding cavitation artifacts.

## 2.2. Time-Resolved Spectroscopic Probes

Structural characterization of protein dynamics requires spectroscopic tools with sufficient time resolution and structural sensitivity. Fluorescence, UV/vis, and IR absorption can follow kinetics down to the picosecond time scale, regardless of the reaction triggering approach (T-jump and other methods reviewed below), since the characteristic times of these spectroscopies are 10–100 fs. The structural specificity of the optical spectroscopies arises from the probing of specific chromophores. For example, emission from the indole ring of a single Trp residue within sizable proteins is easily measured. The structural sensitivity of vibrational spectroscopy is very well established. In general, molecular groups yield well-defined vibrational spectra at specific frequencies and intensities characteristic of the specific group. The accuracy of correlations between vibrational frequencies and key bond properties can be very high. For example, empirical correlations of bond vibrational frequencies have been used in some cases to determine bond lengths to within  $\pm 0.005$  Å, bond orders to within  $\pm 0.04$  valence units, and hydrogen bonding enthalpies to within  $\pm 0.5$  kcal/mol (e.g., ref 59). Protein dynamics can involve changes in protein backbone conformation and H-bonding, in the orientation and packing of side chains, in the solvation of these structures, and so forth, all of which will be reflected in changes in the vibrational spectrum. Two problems have tended to limit the usefulness of IR spectroscopy in the characterization of proteins. One is that water, the natural environment of proteins, absorbs strongly throughout the infrared and has intense absorbance near 3300, 1600, and  $< 800$  cm<sup>-1</sup>. This problem is usually mitigated by the use of D<sub>2</sub>O to access spectral “windows” which are intractable in H<sub>2</sub>O. T-jump relaxation spectrometers can pump either H<sub>2</sub>O or D<sub>2</sub>O. Second, the nearly 10<sup>4</sup> vibrational modes of a typical small protein and the limited frequency dispersion compared to line width combine to produce extreme spectral congestion. Over the past decade, however, revolutionary develop-

ments have occurred in several areas of vibrational technique including difference methods and isotope editing (e.g., ref 59). These developments greatly enhance our ability to assign the vibrational observables to specific structures.

### 2.3. Laser-Induced pH-Jump

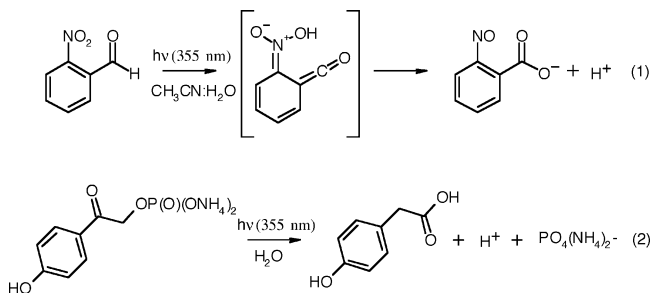
Many enzymatic reactions are pH sensitive, and their equilibria can be shifted by a change in pH. Thus, another approach to the study of fast enzyme dynamics, particularly for reactions involving proton transfer, is the laser-induced pH-jump. The laser-induced pH-jump and its application to proton-transfer dynamics in proteins has been demonstrated by several groups.<sup>60–62</sup> It is well-known that electronically excited states of many organic molecules have different acid–base properties than their ground states. For example, 8-hydroxypyrene-1,3,6-trisulfonate or 2-naphthol-3,6-disulfonate has an excited-state acid dissociation constant ( $pK(S_1) = 0.5$ ) which is much lower than the ground-state value ( $pK(S_0) = 7.0$ ). These compounds effectively emit protons in their excited states. Alternatively, compounds such as the phenylpyridines ( $pK(S_0) = 5$ ,  $pK(S_1) > 10$ ) and acridine ( $pK(S_0) = 5.5$ ,  $pK(S_1) = 10.6$ ) take up protons in the excited state. The efficiencies and kinetics of these processes have been examined in water solution. Gutman and co-workers have examined the dynamics of the proton emitters using short pulsed laser excitation and monitoring the spectral changes of the emitter or of various pH indicators to follow the reaction. Their results indicate that the ejection of protons from the emitters generally occurs within 100 ps and that the rate of protonation of the indicator dye is diffusion controlled.<sup>60</sup> The measured concentration of protons generated was  $10^{-5}$  to  $10^{-4}$  M, using modest dye concentration (100  $\mu$ M) and laser pulse energy (50 mJ). This corresponds to a 3–5 unit decrease in the pH of the solution (e.g. from 7.5 to 4.5). The microsecond duration of the pH-jump is controlled by the recombination of protons with the ground-state ionized proton emitter. The indicator, however, which is protonated during the pulse, remains in its protonated state for a much longer period of time, proportional to its intrinsic acid dissociation constant.

The successful application of the laser-induced pH-jump to enzyme studies has a number of prerequisites. The biochemical inertness of the pH-jump reagent and its ground-state anionic form must be established. The pH-jump reagent must be chosen with a  $pK(S_0)$  matched as closely as possible to the starting pH: in the case of an emitter, the starting pH can obviously not exceed  $pK(S_0)$ ; for an acceptor, the initial pH must be less than  $pK(S_0)$ . In addition, the basicity of the anionic form and its reactions with water or with proton donors from the protein or peptide must be considered. Second, the dynamics of proton emission or uptake and pH equilibration with the protein must be established before the subsequent protein dynamics can be analyzed. A final consideration is the potential interference of the reagent with spectral measurements of the protein dynamics. The viability of the laser-induced pH-jump for the study of enzyme dynamics has been demonstrated by several groups, including our own.<sup>63,64</sup> Furthermore, we have shown that this methodology can be easily coupled with time-resolved IR techniques to probe the protein dynamics.<sup>65</sup>

A different approach is needed to produce a persistent pH-jump, that does not revert to the starting conditions when the system relaxes to the ground state. Persistent pH-jumps have been achieved using photolabile “caged protons”. Thus,

*o*-nitrobenzaldehyde has been used to produce a 1–2 pH unit jump within 50 ns following pulsed laser excitation at 355 nm.<sup>66</sup> UV photolysis of *o*-NBA (*o*-nitrobenzaldehyde) results in an intramolecular redox reaction yielding *o*-nitrosobenzoic acid (Scheme 1). The redox reaction is

**Scheme 1. Photolysis of “caged proton” reagents**



reported to occur with an efficiency of 50% and with a rate constant of  $2 \times 10^9$  s<sup>-1</sup>. Rapid H<sub>2</sub>O addition to the aci-ketene intermediate yields the benzoic acid. Thus, the photochemistry is irreversible and produces a product that does not absorb the pump wavelength and is unreactive with respect to proteins. This caged proton approach has been used to study the kinetics of the pH-induced unfolding of apomyoglobin.<sup>67</sup> The major problem with this particular reagent is its limited solubility in water ( $\sim 500$   $\mu$ M), which restricts the magnitude of the pH-jump which can be produced in the presence of a protein. The buffering capacity of many proteins, for example, together with the  $\sim 100$   $\mu$ M concentration needed for vibrational spectroscopic measurements combine to limit the pH change achievable with this reagent to about 1 unit. We have found that addition of small amounts (0.5%) of CH<sub>3</sub>CN cosolvent greatly increased the solubility of *o*-NBA.

Another class of more soluble “caged proton” reagents is based on *p*-hydroxyphenyl (*p*HP) esters<sup>68,69</sup> (Scheme 1). It is known that several *p*HP esters, including *p*HP ATP and other phosphates, *p*HP glutamate, *p*HP GABA and other carboxylates, and *p*HP mesylate and tosylate, all release the ester group as an acid. The *p*HP chromophore also quantitatively rearranges to a second acid, *p*-hydroxyphenyl acetic acid, thus releasing two new protic acid sites per reacting *p*HP ester. Thus, the reaction effectively releases two protons per photolysis event. These reactions occur with apparent rate constants that approach  $10^8$  s<sup>-1</sup> and with a quantum efficiency between 12 and 20%. These reagents are sufficiently soluble to produce much greater pH-jumps, even in the presence of a significant concentration of protein.

Our work on the dynamics of a model peptide system illustrates the effectiveness of the laser-induced pH-jump as a reaction trigger, particularly when coupled with IR spectroscopy as a structural probe. We used *o*-NBA to generate a persistent pH-jump and IR spectroscopy to follow the structural changes of a helical peptide model, polyglutamic acid.<sup>65</sup> Polyglutamic acid forms a random coil at neutral pH due to the repulsive forces of the ionized carboxylate side chains. However, at low pH ( $pK_a \sim 3.4$ ), as the carboxylate side chains become protonated, the peptide forms an  $\alpha$ -helix. The FTIR difference spectrum following a 266 nm excitation pulse (7 ns, 1 mJ) is shown in Figure 3, overlaid with that of *o*-NBA alone. The short laser pulse generates a 2 pH unit change (from 6.0 to 4.0) within 100 ns. The difference spectra were computed from the spectrum after the flash minus the dark spectrum. Clearly, the pH-

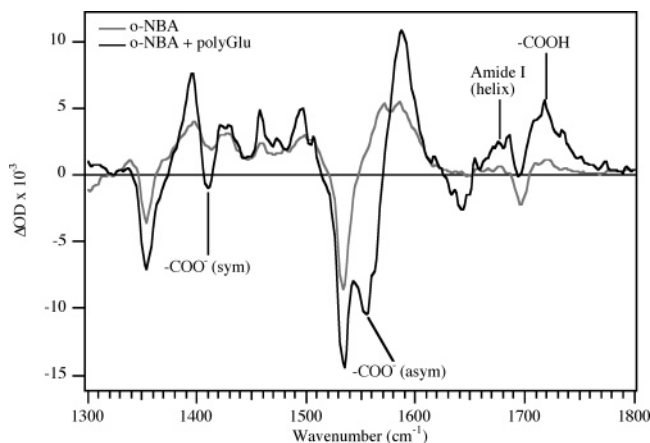


**Figure 3.** FTIR difference spectra of an *o*-NBA + polyglutamic acid mixture following a single 266 nm laser pulse, which induces a pH-jump from 6.0 to 4.0, triggering the coil–helix transition of the polyglutamic acid.

jump initiates two major changes in the polyglutamic acid spectrum. First, the side chains become protonated, as evidenced by the disappearance of the glutamate  $\text{COO}^-$  bands ( $1410\text{ cm}^{-1}$ , sym stretch;  $1555\text{ cm}^{-1}$ , asym stretch) and the appearance of the corresponding protonated band at  $1715\text{ cm}^{-1}$ . Second, the polyglutamic acid becomes helical, as evidenced by the specific shift in the amide I absorbance. In addition, there is evidence from a new peak in the amide I region that the peptide aggregates once it is folded at the concentration used for the FTIR experiments. Furthermore, a kinetics trace obtained at the “marker” position for helix wavelength indicates that the helix is completely formed within the time resolution of the experiment (50 ns). These results demonstrate the viability of the laser-induced pH-jump as an approach to the rapid initiation of protein dynamics, and they also demonstrate the sensitivity of the time-resolved IR approach to the specific structural changes (side chain protonation and backbone conformational changes).

## 2.4. Rapid Mixing Methods

Continuous flow fast mixing methods are perhaps the most general approach to the study of reaction kinetics, although the time resolution of these techniques is limited. These techniques can be applied to any enzymatic reaction by mixing separate enzyme and substrate streams. Since mixing methods rely on diffusion of the enzyme and substrate together, the time resolution is fundamentally limited by the length scale of the mixing process. Two different strategies have been pursued to minimize the mixing length scale and thus to maximize the time resolution of these techniques. The first approach relies on turbulent flow to achieve mixing. The most successful turbulent flow mixer design was developed in 1985 by Clegg and co-workers.<sup>70</sup> This design uses a tapered outer capillary and an inner, smaller-diameter capillary to introduce the two flows to be mixed. A platinum bead is held at the openings of the two capillaries and nearly plugs their outflow. The two sample streams are forced to flow around the sphere at a high flow rate, causing rapid mixing. The mixed stream is then passed through an observation cell, to allow spectroscopic detection of the reaction progress. The fluorescence or absorbance spectrum is obtained as a function of distance along the flow, which can then be converted to time using the flow rate and volume of the flow cell. Using a two-dimensional CCD detector, the

full temporal and spectral response can be recorded simultaneously. The main disadvantage of this approach is the relatively large sample consumption because of the high flow rates needed to produce turbulent flow. Thus, at the fastest time resolution reported for a turbulent flow mixer ( $\sim 50\ \mu\text{s}$ ), the mixer consumes nearly 1 mL of sample per second.<sup>71</sup> The amount of protein required is considerable, depending on the protein concentration and length of signal averaging necessary to produce acceptable signal levels. A number of groups have successfully adapted the Clegg mixer design for the study of protein dynamics, mostly protein folding dynamics.<sup>71</sup> There is one report on the use of this approach to study fast hydride transfer in proton-translocating transhydrogenase (see section 3).<sup>72</sup>

An alternative approach has been developed using microfluidic devices that rely on hydrodynamic focusing of a sample stream, by a surrounding (sheath) stream.<sup>73,74</sup> Because flow rates are much smaller in these devices, the flow is laminar and the sample and sheath streams do not mix. Instead, the reaction is initiated by diffusion of the enzyme substrate into the central sample stream from the sheath flow. We have combined this approach with laser “flash” initiation, using laser photolysis to initiate the reaction. This microfluidics flow-flash experiment is outlined in Figure 4. MbCO

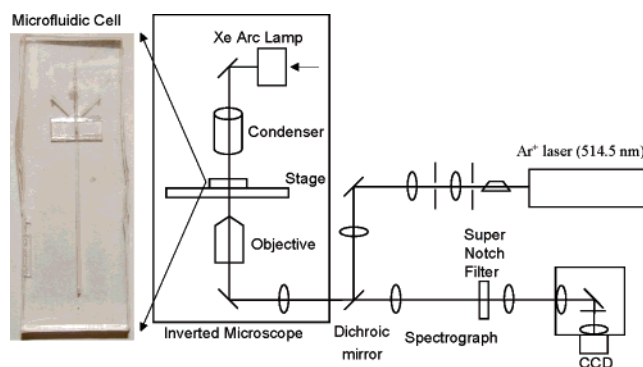


**Figure 4.** Microfluidics flow cell with UV/vis, fluorescence, and Raman detection capabilities.

(myoglobin ligated with carbon monoxide) is placed in the central sample stream, while an oxygenated buffer is used as the sheath flow. Downstream of the hydrodynamic focusing region, the oxygen diffuses into the central sample stream but does not react with Mb, because the reaction is inhibited by the presence of CO. Once the sample stream is equilibrated with  $\text{O}_2$ , a few millimeters downstream from the focusing region, the sample is flowed through a sharply focused, continuous wave laser beam (Ar ion, 514 nm). The laser beam photolyzes the CO and initiates the reaction with  $\text{O}_2$ . The reaction progress is followed by obtaining the full UV/vis absorbance spectrum using a Xe lamp source, an imaging spectrograph, and a CCD detector (Figure 4). The two-dimensional CCD detector records the full spectrum as a function of distance (time) downstream of the laser excitation beam. Thus, the full spectral and temporal response is recorded in a few seconds of integration time, requiring only a few microliters of dilute ( $100\ \mu\text{M}$ ) protein solution. Furthermore, either fluorescence or Raman detection can be implemented with the same instrument design. Microfluidics flow-flash improves the time resolution of the flow experiment to a few microseconds, since it is not limited by the diffusion of reactants together but rather by the spatial resolution of the excitation and detection schemes. The sample requirements are very small, and the approach is

useful for any reaction that can be photochemically initiated.

### 3. Specific Studies

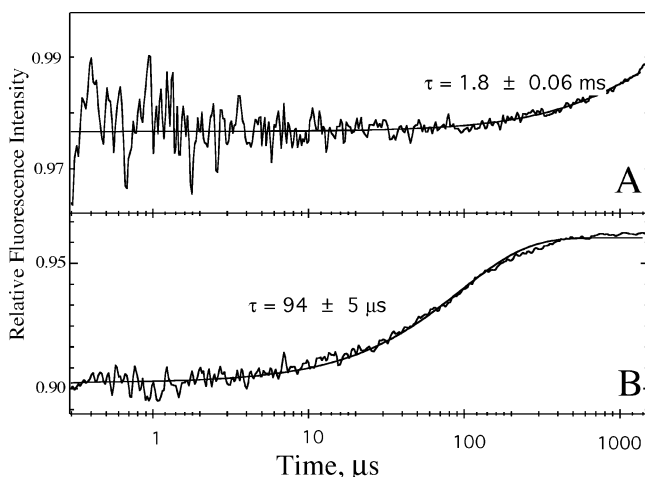
Although just at a very early stage, a sufficient number of studies have been carried out to begin to see the fruitfulness of time-resolved approaches to study the dynamical nature of enzymatic catalysis and also some aspects of their limitations. The results of the few studies performed to date show how little we really understand the dynamical nature of proteins. We summarize the results of studies performed to date.

#### 3.1. Triosephosphate Isomerase (TIM)

##### 3.1.1. Triosephosphate Isomerase (TIM)—A Laser-Induced T-Jump Study

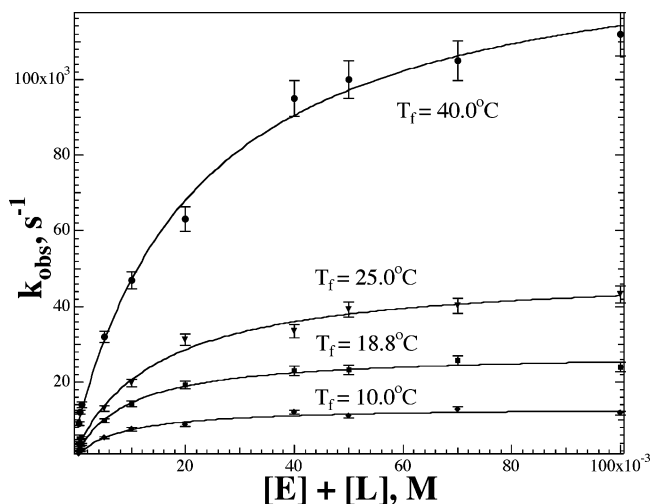
The dynamics of forming the Michaelis complex and the kinetics of ligand binding and loop movement in triosephosphate isomerase (TIM) were characterized using T-jump relaxation spectroscopy coupled with fluorescence of Trp residues as the structural probe.<sup>75</sup> Yeast TIM enzyme contains three Trp residues. One of these, Trp168, is located in the catalytically important surface loop of the enzyme. Since Trp168 is located at the edge of the mobile loop in TIM (residues 166–176) that closes over bound substrate, desolvating the active site and bringing substrate into contact with key protein residues, it was expected that the indole ring emission of this residue would be sensitive to loop closure since the indole ring solvation is significantly modulated during this motion. Accordingly, structural specificity in this study was achieved by constructing a double mutant of *S. cerevisiae* TIM (Trp90Tyr and Trp157Phe) which yields the single Trp containing, Trp168, protein. The TIM (Trp90Tyr and Trp157Phe) mutant has been shown to have identical catalytic properties to those of the wild-type protein.

Figure 5 shows the kinetic response to a 20 °C T-jump of the emission of the indole ring as stimulated in the deep UV and measured at 340 nm of the unligated protein (panel A)



**Figure 5.** Emission, plotted relative to that before the T-jump, at 340 nm in response to a 20 °C T-jump of a solution of 250 μM TIM: (A) unligated TIM; (B) TIM plus 5 mM G3P. The observed responses from 10 to 500 ns (data not shown) and at 1.8 ms do not arise from a response to the binding of a ligand to TIM, but they are likely due to artifacts and due to diffusive cooling of the sample, respectively. TIM, triosephosphate isomerase; G3P, glyceraldehyde 3-phosphate, a nonreactive substrate analogue.

and of TIM in the presence of glyceraldehyde 3-phosphate (G3P), which is a nonreactive substrate analogue (panel B). The only part of the relaxation kinetic profile influenced by the presence of the ligand in panel B is the region from about 1 μs to about 1 ms. For the unligated TIM (panel A), this region is flat, a period of constant intensity, much like the kinetic profile for tryptophan in solution by itself. The relaxation kinetics at 20 °C for TIM ligated with 5 mM G3P in panel B could be fitted to a single-exponential equation and had a lifetime of  $94 \pm 5 \mu\text{s}$ . A detailed study of the TIM–G3P system revealed that the observed relaxation kinetics vary with both the final temperature of the T-jump and the ligand concentration (Figure 6). The higher the final



**Figure 6.** Rate of the relaxation signal in response to a 20 °C T-jump for the TIM + G3P system for various concentrations of free TIM and ligand (i.e., G3P) and temperatures: TIM, triosephosphate isomerase; G3P, glyceraldehyde 3-phosphate, a nonreactive substrate analogue.

jump temperature, the higher is the rate of the single-exponential fit to the relaxation kinetics. Also, as the concentration of the ligand increases, the rate and the amplitude of the relaxation kinetic profile increase.

The variation of the observed rate,  $k_{\text{obs}}$ , with the concentration of free ligand and protein as shown in Figure 6 demonstrates that the observed phenomenon is NOT a simple bimolecular reaction of substrate binding to protein. In that case, the observed rate would scale linearly with concentration; however, saturation was observed. Hence, a kinetic model must include a monomolecular step in addition to the bimolecular encounter reaction. To explain the kinetic data, the following was postulated as the minimal plausible kinetic model, where open and closed refer to the geometry of the loop:



Assuming the initial protein–ligand encounter complex, with TIM in the loop open conformation, forms much more rapidly than the rate of loop closure, which is very likely given the high (mM) concentrations of substrate analogue in these studies, the kinetics of the second step is influenced by the concentrations of free protein and ligand through the concentration of  $\text{TIM}^{\text{open}}/\text{G3P}$ . The following functional form of the rate of the second step, the loop closure step, is derived provided  $k_{\text{on}} \gg k_{\text{open}}$ ,  $k_{\text{closed}}$  (e.g., refs 5, 8, and 49):

$$k_{\text{obs}} = \frac{k_{\text{close}}}{1 + k_{\text{off}}/(k_{\text{on}}\{[\text{TIM}] + [\text{G3P}]\})} + k_{\text{open}}$$

Using this functional form to fit the results of Figure 6 (solid curves), the values of  $k_{\text{open}}$ ,  $k_{\text{close}}$ , and  $k_{\text{on}}/k_{\text{off}}$  are obtained (Table 1).

**Table 1. Rate Constants for the Loop Dynamic in TIM at Different Final Temperatures after the T-Jump**

final temp (°C)	$k_{\text{open}}$ (s <sup>-1</sup> )	$k_{\text{close}}$ (s <sup>-1</sup> )	$k_{\text{off}}/k_{\text{on}}$ (M)
10.0	800 ± 400	12700 ± 600	0.0091 ± 0.0020
18.8	1300 ± 600	26500 ± 700	0.0099 ± 0.0013
25.0	2500 ± 1000	46700 ± 1000	0.0157 ± 0.0026
40.0	8900 ± 1900	(1.31 ± 0.05) × 10 <sup>5</sup>	0.029 ± 0.003

The data support a model in which the rates of the loop opening/closing for TIM are dependent on the ligand, which results in an opening rate in the presence of the product that is comparable to enzymatic throughput,  $k_{\text{cat}}$ . Since the rates were studied as a function of the sample temperature following the jump, a number of thermodynamic conclusions could be reached. The enthalpies of activation of the loop motion,  $\Delta H^{\ddagger}_{\text{close}}$  and  $\Delta H^{\ddagger}_{\text{open}}$ , were estimated to be 13.8 and 14.1 kcal/mol, respectively. Given that the  $\Delta G^{\ddagger}$  values of the opening and closing motions, being on the submillisecond time scale, must be close to the measured enthalpic values, the entropic contributions to both  $\Delta G^{\ddagger}_{\text{close}}$  and  $\Delta G^{\ddagger}_{\text{open}}$  are close to zero. This very interesting result is at first at odds with the notion that the loop may well be quite disordered in the open conformation; it was speculated that the contribution of the changing water structure as the loop motion proceeds needs to be taken into account. The enthalpy of dissociation estimated from the kinetic studies is in reasonable agreement with steady state values. Moreover, the enthalpy was dissected, for the first time, into components associated with ligand binding and with protein conformational change. Perhaps surprising, the overall binding enthalpy of about 9 kcal/mol was found to have a substantial contribution from the formation of the encounter complex, found to contribute 6 kcal/mol of the overall 9 kcal/mol. In contrast, the population ratio of the open to closed loop conformations is found to favor the closed conformation but to be substantially less temperature dependent than the final ligand release step from the encounter complex.

It should be pointed out, even stressed, that similar binding behavior and conclusions have been observed in many enzyme systems (reviewed in refs 8, 76, and 77) in, for example, studies using the T-jump (electrical heating) approaches of Eigen and DeMaeyer.<sup>5</sup> What is new is the substantially enlarged time range that can be probed with the newer techniques, an attribute shown to be important by the TIM studies, and, also, which is illustrated below, a substantially more developed set of structural probes.

### 3.1.2. Triosephosphate Isomerase (TIM)—Comparison of Time-Resolved Results to NMR Relaxation Studies

Since the dynamics of the formation of the Michaelis complex in TIM were studied both by NMR relaxation studies<sup>78,79</sup> and by time-resolved studies (e.g., T-jump, ref 75; see section 3.1.1 above), this offers an opportunity to compare the two methods. The strengths and weaknesses of these two families of methods will sometimes make one more appropriate than the other. NMR spectroscopy can offer

wide-ranging specific structural signatures in connection with the motion; that is, it can report the spatial extent of the motion or offer direct evidence for the structural substates.<sup>10,11</sup> By comparison, the structural specificity of IR absorption spectroscopy, when accompanied by isotope editing techniques, is very specific to specific structural changes and can often be quite well interpreted in terms of underlying interactions; but, this approach is limited to a relatively sparse set of structural probes (to those specific molecules that can be tagged by isotopic labeling, for example). The structural origins of fluorescence changes are often more obscure but, still, for suitably placed chromophoric probes, yield markers of atomic motion at well-defined locations. Both time-resolved and NMR methods have somewhat limited regimes in which they can work: for NMR, substantial populations for the alternative conformation are usually needed, and changes in the NMR chemical shift are required, whereas, for T-jump methods, the states must differ in enthalpy, and changes in IR stretching frequencies and/or fluorescence yield for the two states are essential when optical probes are used as reporters of structural changes. Due to the strong detection sensitivity of especially fluorescence but also IR absorbance, optical relaxation spectroscopy can be highly sensitive to motions on a broad range of time scales (as fast as picoseconds, in principle, and as slow as minutes or longer), including rather small population changes, and thus can be expected to reveal conformational events that are too subtle for NMR methods as well as allowing a more thorough dissection of the kinetic properties, including the thermodynamics of the underlying conformational changes. In the case of the TIM loop motion, both NMR<sup>78,79</sup> and T-jump fluorescence approaches<sup>75</sup> were viable probes of the binding of ligands to the protein. Both yielded the same kinetic mechanism for binding. Both were able to yield the loop opening rate and its temperature dependence quantitatively, and despite many complexities in the ligand dependence, essential agreement between the NMR and the fluorescence derived kinetics was achieved. The T-jump fluorescence approach was able additionally to report on the values of some of the other microscopic rate constants along the binding pathway.

## 3.2. Lactate Dehydrogenase (LDH)—Laser-Induced T-Jump Studies

### 3.2.1. Formation of the LDH/NADH Complex

Laser-induced temperature jump relaxation spectroscopic techniques have been employed to examine the kinetics of NADH binding to lactate dehydrogenase over a nanosecond to millisecond time scale.<sup>80</sup> The bimolecular rate process with an experimental lifetime of 290 μs was easily observed, as were multiple unimolecular faster events (with relaxation times of 200 ns, 3.5 μs, and 24 μs), revealing a rich dynamical nature of the binding step. In solution, measurable populations of intermediates were found whose structures are between ligand and protein unassociated in solution and the bound protein–ligand conformation taken to be the catalytically active one. The results emphasize the dynamic nature of binding and the concept of multiple populated substates of a protein and a protein–ligand system, some of which may well not be functional. The results also emphasize that much is happening on fast times scales which has been, heretofore, largely inaccessible to either experiment or theory. The authors of this study conjectured a view that the binding of NADH to LDH proceeded via the formation of a rather

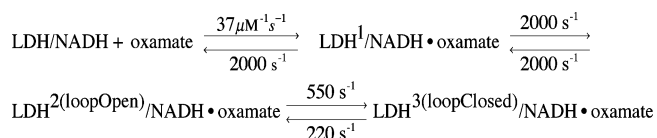
nonspecific structured encounter complex followed by motions whereby, with the adenine moiety anchored to the protein surface, the nicotinamide group works its way into the binding pocket (perhaps the slower 24  $\mu\text{s}$  phase) and, arriving closer to its binding pocket, searches and makes its correct contacts that orient the nicotinamide group properly for the later catalysis steps (the ca. 200 ns and 3.5  $\mu\text{s}$  phases).

### 3.2.2. Formation of the Michaelis Complex in LDH

The Michaelis complex of LDH involves the formation of a ternary complex (LDH/NADH•pyruvate) whereby, in an ordered fashion, LDH binds first NADH and then the substrate pyruvate. Hence, formation of the Michaelis complex can be followed by studying the dynamics of binding LDH/NADH with pyruvate. Studies were recently performed using the substrate surrogate oxamate, so that the observed kinetics do not include any catalyzed chemical steps, via laser-induced T-jump triggering. The evolving structure was monitored from modulations of the fluorescence emission of the reduced nicotinamide group of NADH<sup>56,81</sup> and from changes in the stretching frequencies of key bonds of oxamate, which were identified via isotope edited IR absorption spectroscopy.<sup>82</sup> To access a wide time range, standard stopped-flow kinetic approaches (slower than 1 ms) and laser-induced temperature-jump relaxation spectroscopy (10 ns to 10 ms) were employed; the dynamic range of the combined approaches covered 10 ns to minutes, some 10 orders of magnitude.

Due to the sensitivity of the NADH emission, the binding kinetics could be worked out in detail;<sup>81</sup> the kinetic pathway was verified in the isotope edited IR studies.<sup>82</sup> The results are well explained by a kinetic model that has binding taking place via a sequence of steps: the formation of an encounter complex in a bimolecular step followed by two unimolecular transformations on the microsecond and millisecond time scales (Scheme 2). Details of specific structural transforma-

#### Scheme 2. Formation of the LDH Michaelis complex at 20 °C



tions were well revealed using the IR isotope editing approach. It appears that the various key components of the catalytically competent architecture are brought together as separate events, with the formation of a catalytically key strong hydrogen bonding between active site His195 and substrate early along the binding pathway (occurring on the 500  $\mu\text{s}$  time scale) and the closure of the catalytically necessary protein surface loop over the bound substrate as the final event of the binding process on the several millisecond time scale. This loop remains closed during the entire period that chemistry takes place for native substrates and, as is the case for TIM, loop dynamics limit the observed  $k_{\text{cat}}$ . However, the LDH/NADH•oxamate complex, taken to strongly resemble the Michaelis complex for this protein, consists of a distributed set of conformations interconverting among each other on fast times scales; some of these ternary complexes are not catalytically competent.

It was possible in these studies to obtain all of the microscopic rate constants along the pathway of binding; the on-enzyme  $K_{\text{d}}$  values (the ratios of the microscopic rate

constants for each unimolecular step) are not far from one. Hence, the effective binding constant for the formation of the encounter complex is very close to that of the formation of the catalytically active Michaelis complex. These results reinforce a picture of the physics of enzyme catalysis simultaneously requiring rigidity to maintain close contact between reacting molecules and crucial contacts with active site residues but also flexibility sufficient to get substrates in and out of the binding pocket in a timely fashion. So while the existence of substantial populations of nonactive “Michaelis complexes” seems at first sight inefficient, this may be necessary to permit required entry and leaving of substrates from active sites. It was appreciated that the on-enzyme  $K_{\text{d}}$  values along the binding pathway are not far from one; this appears to be a required design feature of a certain class of enzymes in order to achieve efficient catalytic throughput (see e.g. refs 83 and 84).

Several interesting features of the binding thermodynamics were revealed. It was found that most of the binding enthalpy, about 15 kcal/mol for oxamate binding to LDH/NADH, occurs along with the formation of the crucial strong H-bond between His195 and substrate. The on-rate constant of LDH/NADH with oxamate shows counter Arrhenius behavior, with its value decreasing sharply with temperature up to ca. 40 °C (the highest temperature studied). Moreover, its strongly nonlinear temperature dependence with  $1/T$  is evidence for a large temperature dependence of the activation binding enthalpy,  $\Delta H^{\ddagger}_{\text{kon}}$ . This is a most notable result since the specific heat difference between the transition state and the ground state for forming the LDH/NADH•oxamate encounter complex,  $\Delta C_{\text{p}}^{\ddagger} = 790 \text{ cal}/(\text{mol K})$ , is very large. Such large changes in heat capacity are typically observed in the unfolding of proteins, and the change in heat capacity is generally ascribed to the exposure of hydrophobic residues to water. It was speculated that either substantial, ca. 10–15%, transient melting of the protein or rearrangements of hydrogen bonding and solvent interactions of a number of water molecules, or both, appear to take place to permit substrate access to the protein binding site.

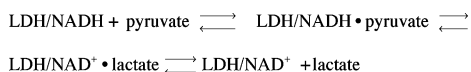
Interestingly, the dynamical nature of how LDH functions, as described by the kinetic results above, appears to be very sensitive to quite specific structural factors, as revealed in studies of the so-called LDH/NAD-pyruvate adduct complex. The essential structural difference between the adduct complex and the true LDH/NADH•pyruvate Michaelis complex is believed to be just the covalent bond between the C4 position of NAD's nicotinamide ring and C3 of pyruvate. Hence, much of the relative motion between the NADH and pyruvate substrates is strongly constrained. This (small) structural change apparently leads to completely different dynamics. A series of T-jump measurements were performed, and shifts in the stretching frequencies of the pyruvate's C=O and COO<sup>-</sup> moieties were monitored by isotope edited IR absorption in the 10 ns to 2 ms time range for the LDH/NAD-pyruvate adduct complex.<sup>56</sup> No motion of any of the active site groups (the bound substrate like moiety or active site residues) was observed even up to temperatures approaching the melting of the protein; it is as if the “freezing” of relative motion between NADH and pyruvate immobilizes the entire active site.

### 3.2.3. Kinetic Processes Associated with On-Enzyme Chemistry and Conformational Changes in LDH

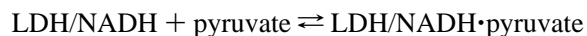
Mixing substrate/product and enzyme in comparable concentrations yields, after coming to equilibrium, bound and

unbound enzyme and substrate/product as well as Michaelis complexes consisting of interconverting enzyme/substrate and enzyme/product productive complexes. For example, when mixing LDH, NAD<sup>+</sup>, and lactate under suitable conditions, the species shown in Scheme 3 are formed in the mixture at equilibrium. At high concentrations of enzyme and cofactor and with an excess of lactate (required to populate the pyruvate side of the reaction since the right-hand side of Scheme 3 is strongly favored at equal

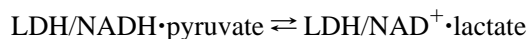
**Scheme 3. Kinetic pathway for the LDH catalyzed chemistry**



concentrations), all the species are well populated.<sup>85</sup> Application of a laser-induced T-jump results in the system coming to a new equilibrium among the species. In this way, chemical events associated with on-enzyme chemistry on time scales faster than milliseconds have been examined for the first time in this enzyme. Monitoring the emission of NADH characterizes the binding event,



since the emission of the dihydronicotinamide group of NADH is heavily quenched when the ternary complex is formed. Following absorption of the NADH dihydronicotinamide headgroup near 340 nm reports directly on the



interconversion since absorbance of NAD<sup>+</sup> at this wavelength is minimal and there is little change in the NADH absorbance when pyruvate binds to LDH/NADH. These experiments are in progress. Preliminary studies of the response as monitored by NADH emission yielded four rates: two near the microsecond time scale and two around 1 ms.<sup>85</sup> The dissociation of pyruvate from LDH/NADH, and loop opening, is observed as a 3.4 ms transient in this study, in agreement with the oxamate studies discussed above (section 3.2.2). The other three events are then assigned to unimolecular events: one near 1 ms and the two faster events at 0.6 and 8 μs. The 1 ms relaxation time is similar to the unimolecular event found in the studies of the substrate surrogate oxamate binding to LDH/NADH (section 3.2.2). It is unclear to what process the two fast events are due. In transient absorption studies (Zhadin and Callender, unpublished data), the chemical step, involving hydride transfer from C4 of NADH to C2 of pyruvate, is resolved for the first time in this enzyme system. At 20 °C the on-enzyme pyruvate–lactate relaxation time is approximately 1.7 ms and shows a primary kinetic H/D isotope effect of about 1.6.

### 3.3. Hydride Transfer in Transhydrogenase—Continuous Flow Rapid Mixing To Resolve the Hydride Transfer Step

Although this section and the next describe studies of time-resolved enzymology with little data on protein dynamics, these recent studies demonstrate nicely applications of newly developed approaches that can probe the connection of dynamics to function in enzymes in ways not heretofore possible. For example, the typical time for the hydride transfer step in redox enzymes that employ NAD(P)H coenzyme lies within the resolution of conventional stopped-

flow devices, about 1 ms. However, this is not always the case. Transhydrogenase, an enzyme found in the inner membranes of animal mitochondria and in the cytoplasmic membranes of many bacteria, catalyzes the hydride transfer between NAD(H) and NADP(H). The hydride transfer step in the enzyme for the NAD<sup>+</sup> to NADPH step is known to be much faster than 1 ms and was resolved recently using a rapid mixing continuous flow device.<sup>86</sup> The reporter for the chemical step was Trp fluorescence coming from mutant enzyme whereby a single Trp residue was judiciously incorporated into the protein. The first order on-enzyme rate constant was found to be 21 200 s<sup>-1</sup> with a primary kinetic H/D isotope effect of approximately 2.

### 3.4. Hydrolysis Reaction of the Ras Protein—The Use of Caged Compounds

Ras is a cellular messenger whose importance in mammalian tumorigenesis has resulted in intensive studies of its function at the molecular, cellular, and organismic levels. Ras plays essential roles in regulating the cell cycle, apoptosis, mitogen-activated protein kinase pathways, and retroviral activation. Ras binds both GDP and GTP, and it is active in the GTP form. The allosteric interactions that mediate signaling between GTPases and their targets are typically switched from on to off by the on-enzyme hydrolysis of GTP. Hence, the structures of the Ras/GDP and Ras/GTP forms, the interconversion between these two species, and the complexes of Ras with other compounds or proteins that affect the on-enzyme rate of GTP hydrolysis are all important. Crystallographic<sup>87–92</sup> and vibrational<sup>93–96</sup> structures of Ras/GTP and Ras/GDP have been studied in steady-state non-time-resolved investigations. In these cases, the labile Ras/GTP species can be characterized either by working at low temperatures (near 0 °C) where the hydrolysis reaction is slowed or via the use of nonhydrolyzable GTP analogues. Several time-resolved studies have been performed using caged GTP as a photochemical trigger in both crystallographic and FTIR studies.

#### 3.4.1. Time-Resolved Crystallographic Studies

Caged GTP was found to cocrystallize well with the Ras protein. Crystallographic data were taken on the caged GTP/Ras complex, the hydrolysis reaction was initiated by light in the 300–400 nm range, and the time dependence of the reaction was followed.<sup>33,40,97</sup> The structure refinements showed that the structure of the Ras/GTP Michaelis complex is similar to those of complexes of Ras with nonhydrolyzable GTP analogues and that the on-enzyme hydrolysis reaction proceeds in the same manner for crystal complexes of Ras/GTP as it does for protein–nucleotide complexes in solution. No kinetic intermediate from Ras/GTP to Ras/GDP + Pi was found to accumulate.

#### 3.4.2. Time-Resolved FTIR Studies

In the time-resolved vibrational studies,<sup>98,99</sup> the caged GTP bound to Ras was irradiated (typically in the near UV), releasing GTP from the cage in around 90 ms (see refs 31 and 34 for overviews). The hydrolysis reaction was then probed as a function of time by FTIR spectroscopy using a FTIR spectrometer in rapid scan mode. Difference spectra are formed from the resulting IR spectra at various time points and report on the reaction and the absorbance changes of the involved groups, either protein or bound nucleotide.

To assign the phosphate modes of the bound nucleotide, the phosphate groups were labeled with  $^{18}\text{O}$  and parallel studies were performed. In this way, the changes in structure as Ras/GTP evolves to Ras/GDP were studied. The first study of this kind was ref 100. More recent studies<sup>98,99</sup> with improved methodologies have yielded substantial improvements in signal-to-noise. It was found that binding of GTP to Ras affects the electronic distribution and structure of the phosphate groups, with negative charge shifting toward the  $\beta$ -phosphate as the hydrolysis reaction proceeds in addition to a number of other structural changes.<sup>99</sup> The Ras on-enzyme hydrolysis reaction is greatly accelerated by the interaction of Ras with GAP (GTPase activating protein). Time-resolved studies of the GAP·Ras catalyzed reaction suggested that the mechanism underlying the hydrolysis reaction may differ to some extent from that of the intrinsic GTPase reaction of Ras.<sup>98</sup> The GAP/Ras reaction involves an intermediate, not found in the Ras reaction, in which the  $\gamma$ -phosphate of GTP is cleaved but remains within the binding pocket. The bridging  $\beta$ -bond (GDP–Pi) frequency of GTP is downshifted in Ras compared to GTP in solution, and it is even more downshifted in GAP·Ras. The authors suggested that this shift is due to charge polarization caused by the presence in the active site of an Arg group provided by the GAP protein.<sup>31,98</sup> Similar work has recently been performed on Rap1,<sup>101</sup> a close relative to the Ras protein in both structure and function. The intrinsic hydrolysis reactions of the two proteins seem to be similar and yield similar shifts of charge to the  $\beta$ -phosphate. The GAP catalyzed reactions show unique features. The binding pattern of the phosphate groups of GTP in GAP·Ras differs from that of GAP·Rap, which, it is speculated, compensates for the absence of a *cis*-Gln (found in Ras) by a *trans*-Asn (found in Rap), resulting in a bound GTP more prone to attack by a structural water molecule.

#### 4. Acknowledgment

This work was supported by the Institutes of General Medicine and Biomedical Imaging and Bioengineering of the National Institutes of Health (Grants GM068036 and EB01958).

#### 5. References

- (1) Koshland, D. E. *Proc. Natl. Acad. Sci., USA* **1958**, *44*, 98.
- (2) Michaelis, L.; Menten, M. L. *Biochem. Z.* **1913**, *49*, 333.
- (3) Roughton, F. J. W. *Proc. R. Soc.* **1934**, *B115*, 475.
- (4) Chance, B. *J. Franklin Inst.* **1940**, *229*, 455.
- (5) Eigen, M.; DeMaeyer, L. D. In *Technique of Organic Chemistry*; Friess, S. L., Lewis, E. S., Weissberger, A., Eds.; Interscience: New York, 1963; Vol. 8, pp 895–1054.
- (6) Eigen, M.; Hammes, G. G. *Adv. Enzymol.* **1963**, *25*, 1.
- (7) Hammes, G. G. *Adv. Protein Chem.* **1968**, *23*, 1.
- (8) Hammes, G. G.; Schimmel, P. R. In *The Enzymes*, 3rd ed.; Boyer, P. D., Ed.; Academic Press: New York, 1970; Vol. II, pp 67–114.
- (9) Antoniou, D.; Basner, J. E.; Nunez, S.; Schwartz, S. D. *Chem. Rev.* **2006**, *106*, pp 3170–3187.
- (10) Palmer, A. G., III. *Chem. Rev.* **2004**, *104*, 3623.
- (11) McDermott, A. E. *Curr. Opin. Struct. Biol.* **2004**, *14*, 554.
- (12) Schnell, J. R.; Dyson, H. J.; Wright, P. E. *Annu. Rev. Biophys. Biomol. Struct.* **2004**, *33*, 119.
- (13) Deleted in proof.
- (14) Min, W.; English, B. P.; Luo, G.; Cherayil, B. J.; Kou, S. C.; Xie, X. S. *Acc. Chem. Res.* **2005**, *38*, 923.
- (15) Smiley, R. D.; Hammes, G. *Chem. Rev.*, published online May 27, 2006, <http://dx.doi.org/10.1021/cr0502955>, pp 3080–3094.
- (16) Denisov, I. G.; Makris, T. M.; Sliker, S. G.; Schlichting, I. *Chem. Rev.* **2005**, *105*, 2253.
- (17) McMahon, B. H.; Fabian, M.; Tomson, F.; Causgrove, T. P.; Bailey, J. A.; Rein, F. N.; Dyer, R. B.; Palmer, G.; Gennis, R. B.; Woodruff, W. H. *Biochim. Biophys. Acta* **2004**, *1655*, 321.
- (18) Gennis, R. B. *Front. Biosci.* **2004**, *9*, 581.
- (19) Nienhaus, K.; Nienhaus, G. U. In *Protein–Ligand Interactions: methods and applications*; Nienhaus, G. U., Ed.; Humana Press: Totowa, NJ, 2005; Vol. 305, pp 215–242.
- (20) Lim, M.; Anfinrud, P. In *Protein–Ligand Interactions: methods and applications*; Nienhaus, G. U., Ed.; Humana Press: Totowa, NJ, 2005; Vol. 305, pp 243–260.
- (21) Samuni, U.; Friedman, J. M. In *Protein–Ligand Interactions: methods and applications*; Nienhaus, G. U., Ed.; Humana Press: Totowa, NJ, 2005; Vol. 305, pp 115–154.
- (22) Nibbering, E. T. J.; Fidler, H.; Pines, E. *Annu. Rev. Phys. Chem.* **2005**, *56*, 337.
- (23) Arnett, D. C.; Moser, C. C.; Dutton, P. L.; Scherer, N. F. *J. Phys. Chem. B* **1999**, *103*, 2014.
- (24) Callender, R.; Gilmanshin, R.; Dyer, R. B.; Woodruff, W. *Physics World*; Institute of Physics: Bristol, England, 1994; Vol. 7, pp 41–45.
- (25) Williams, S.; Causgrove, T. P.; Gilmanshin, R.; Fang, K. S.; Callender, R.; Woodruff, W.; Dyer, R. B. *Biochemistry* **1996**, *35*, 691.
- (26) Phillips, C. M.; Mizutani, Y.; Hochstrasser, R. M. *Proc. Natl. Acad. Sci., U.S.A.* **1995**, *92*, 7292.
- (27) Ballew, R. M.; Sabelko, J.; Gruebele, M. *Nat. Struct. Biol.* **1996**, *3*, 923.
- (28) Thompson, P. A.; Eaton, W. A.; Hofrichter, J. *Biochemistry* **1997**, *36*, 9200.
- (29) Pasher, T.; Chesick, J. P.; Winkler, J. R.; Gray, H. B. *Science* **1996**, *271*, 1558.
- (30) Park, C. H.; Givens, R. S. *J. Am. Chem. Soc.* **1997**, *119*, 2453.
- (31) Kottling, C.; Gerwert, K. *ChemPhysChem* **2005**, *6*, 881.
- (32) Scheidig, A. J.; Burmester, C.; Goody, R. S. *Methods Enzymol.* **1998**, *291*, 251.
- (33) Schlichting, I.; Almo, S. C.; Rapp, G.; Wilson, K.; Petratos, K.; Lentfer, A.; Wittinghofer, A.; Kabsch, W.; Pai, E. F.; Petsko, G. A.; Goody, R. S. *Nature* **1990**, *345*, 309.
- (34) Kottling, C.; Gerwert, K. In *Protein–Ligand Interactions: methods and applications*; Nienhaus, G. U., Ed.; Humana Press: Totowa, NJ, 2005; Vol. 305, pp 261–286.
- (35) EllisDavies, G. C. R.; Kaplan, J. H.; Barsotti, R. J. *Biophys. J.* **1996**, *70*, 1006.
- (36) Takahashi, S.; Yeh, S. R.; Das, T. K.; Chan, C. K.; Gottfried, D. S.; Rousseau, D. L. *Nat. Struct. Biol.* **1997**, *4*, 44.
- (37) Shastry, M. C. R.; Luck, S. D.; Roder, H. *Biophys. J.* **1998**, *74*, 2714.
- (38) Knight, J. B.; Vishwanath, A.; Brody, J. P.; Austin, R. H. *Phys. Rev. Lett.* **1998**, *80*, 3863.
- (39) Roder, H.; Maki, K.; Cheng, H.; Shastry, M. C. R. *Methods* **2004**, *34*, 15.
- (40) Schlichting, I.; Goody, R. S. *Methods Enzymol.* **1997**, *277*, 467.
- (41) Stoddard, B. L.; Cohen, B. E.; Brubaker, M.; Mesecar, A. D.; Koshland, D. E. *Nat. Struct. Biol.* **1998**, *5*, 891.
- (42) Schmidt, M.; Ihee, H.; Pahl, R.; Srajer, V. In *Protein–Ligand Interactions: methods and applications*; Nienhaus, G. U., Ed.; Humana Press: Totowa, NJ, 2005; Vol. 305, pp 115–154.
- (43) Carey, P. R.; Dong, J. *Biochemistry* **2004**, *43*, 8885.
- (44) Beitz, J. V.; Flynn, G. W.; Turner, D. H.; Sutin, N. *J. Am. Chem. Soc.* **1970**, *92*, 4130.
- (45) Anfinrud, P. A.; Han, C.; Hochstrasser, R. M. *Proc. Natl. Acad. Sci., U.S.A.* **1989**, *86*, 8387.
- (46) Richard, L.; Genberg, L.; Deak, J.; Chiu, H.-L.; Miller, R. J. D. *Biochemistry* **1992**, *31*, 10703.
- (47) Bernasconi, C. F. *Relaxation Kinetics*; Academic Press: New York, 1976.
- (48) Cantor, C. R.; Schimmel, P. R. *Biophysical Chemistry*; W. H. Freeman and Company: San Francisco, 1980; Chapter 16.
- (49) Fersht, A. *Structure and Mechanism in Protein Science: A Guide to Enzyme Catalysis and Protein Folding*; Freeman and Co.: New York, 1999; Chapter 4.
- (50) Hoffmann, H.; Yeager, E.; Stuehr, J. *Rev. Sci. Instrum.* **1968**, *39*, 649.
- (51) Turner, D. H.; Flynn, G. W.; Sutin, N.; Beitz, J. V. *J. Am. Chem. Soc.* **1972**, *94*, 1554.
- (52) Smith, J. J.; McCray, J. A.; Hibberd, M.; Ye, G. *Rev. Sci. Instrum.* **1989**, *60*, 231.
- (53) Holwarth, J.; Schmidt, A.; Wolff, H.; Volk, R. *J. Phys. Chem.* **1977**, *81*, 22.
- (54) Chen, S.; Lee, S.; Tolbert, W. A.; Wen, X.; Dlott, D. D. *J. Phys. Chem.* **1992**, *96*, 7178.
- (55) Dyer, R. B.; Gai, F.; Woodruff, W. H.; Gilmanshin, R.; Callender, R. H. *Acc. Chem. Res.* **1998**, *31*, 709.

- (56) Gulotta, M.; Deng, H.; Deng, H.; Dyer, R. B.; Callender, R. H. *Biochemistry* **2002**, *41*, 3353.
- (57) Vu, D. M.; Peterson, E. S.; Dyer, R. B. *J. Am. Chem. Soc.* **2004**, *126*, 6546.
- (58) Wray, W. O.; Aida, T.; Dyer, R. B. *Appl. Phys. B: Lasers Opt.* **2002**, *74*, 57.
- (59) Callender, R.; Deng, H. *Annu. Rev. Biophys. Biomol. Struct.* **1994**, *23*, 215.
- (60) Gutman, M.; Huppert, D.; Pines, E. *J. Am. Chem. Soc.* **1981**, *103*, 3709.
- (61) Gutman, M.; Nachliel, E. *Annu. Rev. Phys. Chem.* **1997**, *48*, 329.
- (62) Iu, K.-K.; Kuczynski, J.; Fuerniss, S. J.; Thomas, J. K. *J. Am. Chem. Soc.* **1992**, *114*, 4871.
- (63) Marantz, Y.; Einarsdottir, O.; Nachliel, E.; Gutman, M. *Biochemistry* **2001**, *40*, 15086.
- (64) Marantz, Y.; Nachliel, E.; Aagaard, A.; Brzezinski, P.; Gutman, M. *Proc. Natl. Acad. Sci., U.S.A.* **1998**, *95*, 8590.
- (65) Causgrove, T. P.; Dyer, R. B. *Chem. Phys.* **2006**, *323*, 2.
- (66) Viappiani, C.; Bonetti, G.; Carcelli, M.; Ferrari, F.; Sternieri, A. *Rev. Sci. Instrum.* **1998**, *69*, 270.
- (67) Abbruzzetti, S.; Crema, E.; Masino, L.; Vecli, A.; Viappiani, C.; Small, J. R.; Libertini, L. J.; Small, E. W. *Biophys. J.* **2000**, *78*, 405.
- (68) Givens, R. S.; Jung, A.; Park, C. H.; Weber, J.; Bartlett, W. *J. Am. Chem. Soc.* **1997**, *119*, 8369.
- (69) Givens, R. S.; Weber, J. F. W.; Conrad, P. G.; Orosz, G.; Donahue, S. L.; Thayer, S. A. *J. Am. Chem. Soc.* **2000**, *122*, 2687.
- (70) Regenfuss, P.; Clegg, R. M.; Fulwyler, M. J.; Barrantes, F. J.; Jovin, T. M. *Rev. Sci. Instrum.* **1985**, *56*, 283.
- (71) Roder, H.; Maki, K.; Cheng, H.; Shastry, M. C. R. *Methods (Amsterdam)* **2004**, *34*, 15.
- (72) Pinheiro, T. J. T.; Venning, J. D.; Jackson, J. B. *J. Biol. Chem.* **2001**, *276*, 44757.
- (73) Hertzog, D. E.; Michalet, X.; Jäger, M.; Kong, X.; Santiago, J. G.; Weiss, S.; Bakajin, O. *Anal. Chem.* **2004**, *76*, 7169.
- (74) Pollack, L.; Tate, M. W.; Darnton, N. C.; Knight, J. B.; Gruner, S. M.; Eaton, W. A.; Austin, R. H. *Proc. Natl. Acad. Sci., U.S.A.* **1999**, *96*, 10115.
- (75) Desamero, R.; Rozovsky, S.; Zhadin, N.; McDermott, A.; Callender, R. *Biochemistry* **2003**, *42*, 2941.
- (76) Gutfreund, H. *Annu. Rev. Biochem.* **1971**, *40*, 315.
- (77) Cantor, C. R.; Schimmel, P. R. *Biophysical Chemistry*; W. H. Freeman and Company: San Francisco, 1980; pp 921–922.
- (78) Rozovsky, S.; McDermott, A. E. *J. Mol. Biol.* **2001**, *310*, 259.
- (79) Rozovsky, S.; Jogl, G.; Tong, L.; McDermott, A. E. *J. Mol. Biol.* **2001**, *310*, 271.
- (80) Deng, H.; Zhadin, N.; Callender, R. *Biochemistry* **2001**, *40*, 3767.
- (81) McClendon, S.; Vu, D.; Callender, R.; Dyer, R. B. *Biophys. J.* **2005**, *89*, L07.
- (82) McClendon, S.; Zhadin, N.; Callender, R. *Biophys. J.* **2005**, *89*, 2024.
- (83) Burbaum, J. J.; Knowles, J. R. *Biochemistry* **1989**, *28*, 9306.
- (84) Brubau, J. J.; Raines, R. T.; Alberly, W. J.; Knowles, J. R. *Biochemistry* **1989**, *28*, 9293.
- (85) Callender, R.; Dyer, R. B. *Curr. Opin. Struct. Biol.* **2002**, *12*, 628.
- (86) Pinheiro, T. J. T.; Venning, J. D.; Jackson, J. B. *J. Biol. Chem.* **2001**, *276*, 44757.
- (87) Wittinghofer, A.; Pai, E. *Trends Biochem. Sci.* **1991**, *16*, 382.
- (88) Tong, L.; de Vos, A. M.; Milburn, M. V.; Kim, S. H. *J. Mol. Biol.* **1991**, *217*, 503.
- (89) Pai, E. F.; Krengel, U.; Petsko, G. A.; Goody, R. S.; Kabsch, W.; Wittinghofer, A. *EMBO J.* **1990**, *9*, 2351.
- (90) Wittinghofer, A.; Krengel, U.; John, J.; Kabsch, W.; Pai, E. F. *Environ. Health Perspect.* **1991**, *11*.
- (91) Franken, S. M.; Scheidig, A. J.; Krengel, U.; Rensland, H.; Lautwein, A.; Geyer, M.; Scheffzek, K.; Goody, R.; Kalbitzer, H. R.; Pai, E.; Wittinghofer, A. *Biochemistry* **1993**, *32*, 8411.
- (92) Scheffzek, K.; Ahnadian, M. R.; Kabsch, W.; Wiesmuller, L.; Lautwein, A.; Schmitz, F.; Wittinghofer, A. *Science* **1997**, *277*, 333.
- (93) Manor, D.; Weng, G.; Deng, H.; Cosloy, S.; Chen, C. X.; Balogh-Nair, V.; Delaria, K.; Jurnak, F.; Callender, R. H. *Biochemistry* **1991**, *30*, 10914.
- (94) Wang, J. H.; Xiao, D. G.; Deng, H.; Webb, M. R.; Callender, R. *Biochemistry* **1998**, *37*, 11106.
- (95) Cheng, H.; Sukal, S.; Callender, R.; Leyh, T. *J. Biol. Chem.* **2001**, *276*, 9931.
- (96) Cheng, H.; Sukal, S.; Deng, H.; Leyh, T. S.; Callender, R. *Biochemistry* **2001**, *40*, 4035.
- (97) Schlichting, I.; Papp, G.; John, J.; Wittinghofer, A.; Pai, E.; Goody, R. S. *Proc. Natl. Acad. Sci., U.S.A.* **1989**, *86*, 7687.
- (98) Allin, C.; Ahmadian, M. R.; Wittinghofer, A.; Gerwert, K. *Proc. Natl. Acad. Sci., U.S.A.* **2001**, *98*, 7754.
- (99) Allin, C.; Gerwert, K. *Biochemistry* **2001**, *40*, 3037.
- (100) Cepus, V.; Goody, R. S.; Gerwert, K. *Biochemistry* **1998**, *37*, 10263.
- (101) Chakrabarti, P.; Suveyzdis, Y.; Wittinghofer, A.; Gerwert, K. *J. Biol. Chem.* **2004**, *279*, 46226.

CR050284B